Team WORX: Design and Development of an Autonomous USV for RobotX, The Inaugural Maritime Challenge, Singapore 2014

TEAM WORX

A. Lebbad (VU), E. Sarda (FAU), J. Anderson (VU), I. Bertaska (FAU), M. Miranda (FAU), M. Benson (VU), G. Cheng (VU), D. DeGaetano (VU), K. Haizlett (FAU), J. Lapix (FAU), A. Long (FAU), J. Martinez (FAU), B. Mesa (FAU), T. Moscicki (FAU), E. Zhu (VU), G. Clayton (VU), K. von Ellenrieder (FAU), C. Nataraj (VU)

Abstract

This article presents an overview of the systems developed and equipped on a WAM-V USV16 (16 foot Wave Adaptive Modular Vehicle), and pioneered by a team of students from both Villanova University and Florida Atlantic University. The vessel uses an extensive sensor suite including a RGB-D vision system robust to lighting variations, an underwater USBL (Ultra Short Base Line) localization system, and a GPS aided MEMS-based Inertial Measurement Unit. Many innovative technologies, which have been developed for the first time ever, have been implemented on the vehicle. For example, the developed controller is robust to various environmental disturbances, including wind force, current, lighting variations, and rain, and the vision system implements a novel data fusion algorithm and integrates an innovative Bayesian color recognition. Team WORX's WAM-V USV16 carries out three degree of freedom state estimation, mapping, path planning, obstacle avoidance and navigation. Mission-level control is provided by a hierarchical structure and programmed using a finite state machine, allowing for the development of modular routines that can be rapidly implemented.

I. Introduction

The AUVSI Foundation and the Office of Naval Research have established the Maritime RobotX Challenge, an international competition intended to foster student interest in autonomous marine robotic systems. This style of scientific challenge provides students a real-world experience of having to meet a distinct set of engineering objectives within allotted timeframe, requiring the students to come together as a team to rapidly develop such a system. The tasks include the ability to show: 1) vehicle propulsion strength and speed; 2) the agility to visually navigate through a buoy field; 3) home to a localized source with an underwater navigation system; 4) correctly locate and report objects of interest such as a light sequence; 5) locate and park the vehicle within a designated docking slip; and 6) make way back to a starting, home position; all without human interaction or involvement.

As one of three teams selected to represent the United States in this competition, Villanova University (VU) and Florida Atlantic University (FAU) have created a partnership that leverages Villanova's skill in visual perception and high level control and FAU's proficiency in systems integration, underwater acoustics and navigation, control, and platform development. The team consists of students and faculty from both institutions, working together to address the technical and logistical challenges of the RobotX competition.

II. Design Overview

A systems engineering approach has been applied for the design and development of the vehicle's Guidance, Navigation & Control (GNC) system, as well as a unique propulsion system implementation. Inspired by the mission challenges, a detailed exploration of the available sensors and their capabilities was thoroughly carried out for their selection process.

The vehicle's onboard systems can be broken down into four major components: a high-level mission management and path planning controller (developed by VU), a vision-based perception system (developed by VU), low-level thrust allocation controller with a three degree of freedom state estimator (developed by FAU), and an underwater acoustic tracking and positioning SONAR (Sound Navigation and Ranging) system with real-time motion compensation and automated launch and recovery system (developed by FAU). The combination of sensor instrumentation includes an onboard camera fused with a LIDAR (Light Detection and Ranging) for 3D spatial and color identification used to map the surface environment, GPS for global vehicle positioning, inertial measurement unit (IMU) including accelerometers and gyroscope to measure vehicle motion, and an ultra-short baseline (USBL) SONAR array for underwater source localization.

The high-level vehicle planner with vision navigation system is interfaced with the low-level controller and the underwater SONAR system through a multi-cast UDP Ethernet network known as the Lightweight Communications and Marshalling (LCM) System. Each subsystem is controlled using dedicated central processing units (CPUs) to accommodate the required processing speeds and resources. This layered architecture approach provides modularity to the subsystems, allowing them to work independently at precise update rates to provide the highest system resolution.

The vehicle has a Singaporean compatible WiFi access point and RF modem for wireless communication to a shore-based user. There are also three different dedicated lead-acid power systems on board, including independent power for port and starboard thrusters respectively, and independent hotel power for the vehicle's computer systems and instrumentation. Power systems for each propulsion thruster are also equipped with

emergency shutoff switches in case there is the need of emergency demobilization. Figure 1 below shows a functional block diagram of the vehicle's guidance, navigation and control system.

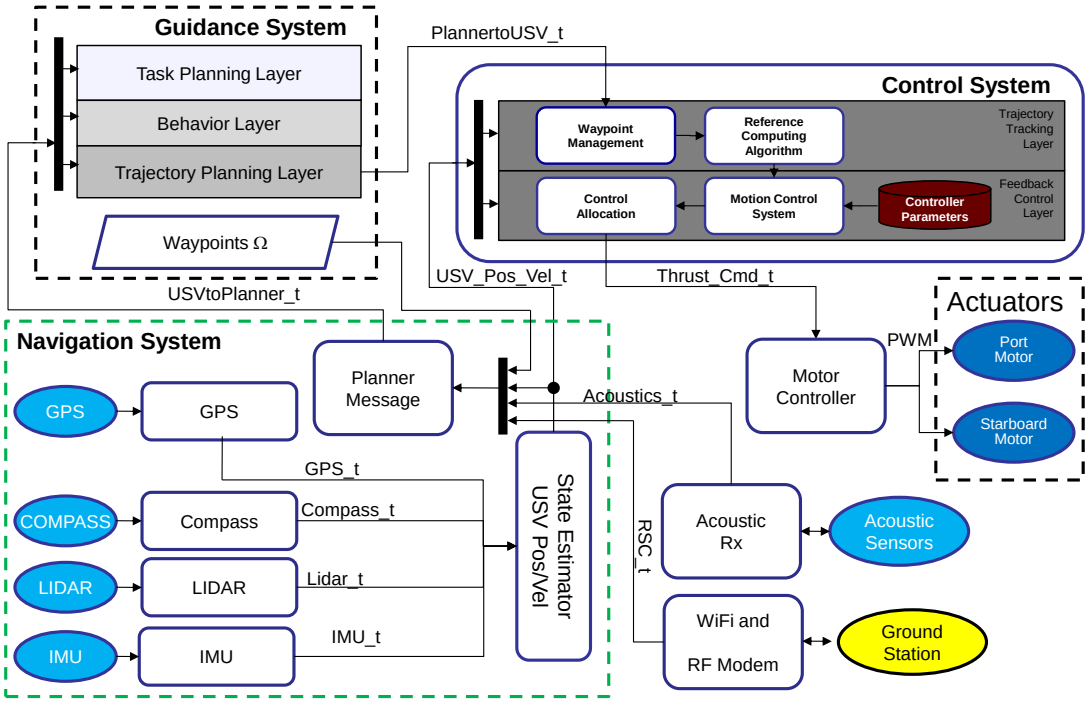

Figure 1: Guidance, Navigation and Control System.

III. Vehicle Platform

The WAM-V USV16 was provided by the Office of Naval Research and Marine Advanced Research, and is the same vehicle used by all teams in the competition. The WAM-V USV16 is a catamaran style vessel, designed to work best with differential thrust propulsion systems for maximum maneuverability. In particular, what makes the WAM-V USV16 so unique is the independent suspension system installed on each of its hulls. The suspension system provides superior stability of the payload deck and dampens vibration that can cause unnecessary instrumentation noise during transit due to the vehicle's motion response when coupled with surface wave interaction (Figure 2).

Figure 2: WAM-V USV16 during ocean tests.

Upon delivery of the vehicle, the team was required to design and develop an entirely custom propulsion system that is capable of interfacing with the vehicle's navigation and control systems. The propulsion consists of two 12 Volt Minn Kota Riptide III electric thrusters and custom mounting brackets, located on each hull (Figure 3). Each motor can output a peak thrust of 245 Newtons, allowing the vehicle to robustly navigate a sequence of points along a desired trajectory. The required force output by each propeller, which allows the vehicle to maneuver, is dictated by the trajectory tracking controller (see section VI.).

The vehicle was originally designed to be equipped with extended bulkheads attached to the aft end of each hull. When thrusters are attached directly to the transom without the extended bulkheads, the vehicle tends to lose buoyancy in the stern, which causes the bow of each hull to pitch upward. As a solution to the problem, end caps, made out of marine high density foam (Figure 3), were also added as part of the design to recover the lost buoyancy at the aft end of each hull. These end caps also reduce flow separation at the stern during forward motion thus improving the USV16's hydrodynamic efficiency.

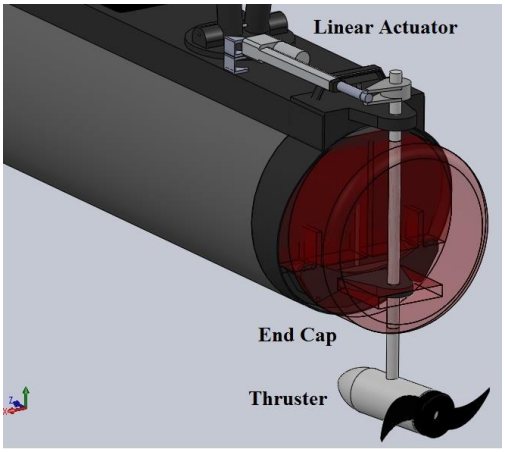

Figure 3: CAD drawing of propulsion system located on each hull.

The propulsion system also utilizes two 6 inch (15 cm) stroke Firgelli linear actuators to allow control over the direction of the thrust (Figure 4). By varying the thrust direction, the vehicle is capable of maintaining a desired position and heading, without the need for an anchor. The station keeping controller (section VI) makes this possible by controlling the output thrust and its direction.

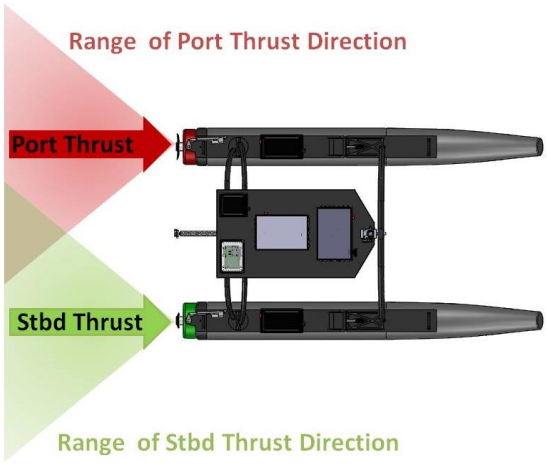

Figure 4: Differential thrust illustration on WAM-V USV16.

IV. Layered Software Architecture

The system's layered design essentially provides independent and parallel control for each subsystem on the platform. The software architecture of the vehicle uses a finite state machine (FSM) that schedules and manages the mission objectives [16].

Using defined priority allocation to the mission, each objective is attempted as a set of defined tasks which are carried out by organized processes, or "threads". Several programs are independently run to manage these processes and are linked together using an extensive communication bus.

High-level state messages are used to work with middle-layer programs that control general vehicle components (e.g. navigation, data filtering, data logging) and house-keeping functions (e.g. mission timers, and communication to the user).

V. Navigation Systems

V.I Vision System:

Computer vision is an invaluable capability for autonomous surface vehicles (ASVs), or any autonomous vehicle for that matter. This is primarily due to the large amount of unique information contained in images. The advantage of a LIDAR/Video vision system is that, in addition to typical camera information, such as color, morphology, and the angular location of objects within the camera's field of view (FOV), depth information is also available. Depth is extremely important for ASVs, as it enables the use of advanced vision algorithms like simultaneous localization and mapping (SLAM) and object based color analysis [4].

The Maritime RobotX Challenge is uniquely difficult, requiring the ASV to autonomously complete a number of tasks including visual obstacle identification, obstacle avoidance and docking. This level of autonomy is achieved, in part by using the LIDAR/Video vision system mounted on a rotating gimbal, shown in Figure 5. The LIDAR scanner (Hokuyo UTM-30LX) scans on a plane and is used to obtain distance information while the video camera (Logitech Pro 9000) is used to obtain color and morphological information about the objects in the vision system's FOV.

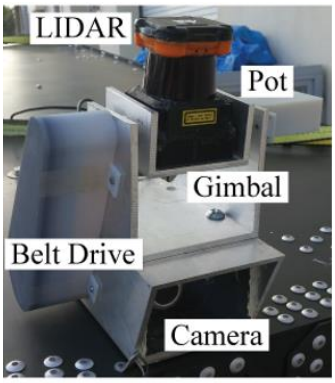

Figure 5: The LIDAR/Video vision system.

LIDAR systems capable of achieving a two dimensional depth map are quite expensive. An alternative used in this system is a lower cost, planar LIDAR system (that is, a LIDAR that collects range information from one plane in the scene being measured). The sensing can then be extended to 3D by adding secondary rotation to the sensor [1,6,12,13].

The primary mechanical component of the vision system is a gimbal that enables LIDAR scanning. The LIDAR sensor only collects data on a single plane, thus necessitating this rotation. As shown, the LIDAR device is mounted on a rotating cradle. The cradle is mounted on a waterproof box that houses the forward-looking camera, as well as a stepper motor (NEMA-17 with a 14:1 gearbox) which actuates the gimbal through a belt. Additional components include a potentiometer which allows measurement of the gimbal angle and waterproof covers for the potentiometer and timing belt, which were produced using a 3D printer.

The stand-alone vision system is designed with the capability to control the gimbal, measure data, and perform image-processing. The primary computational resource for this task is a Pandaboard single board computer running a Linux operating system. The Pandaboard is programmed using MathWorks' Simulink and Real Time Workshop packages. Both the Hokuyo LIDAR device and the Logitech camera are connected directly to the Pandboard. The stepper motor used to control the gimbal is driven by a Phidgets 1067 control board and the gimbal angle is measured using a potentiometer read by an Arduino UNO. Both the stepper driver and the Arduino are connected to the Pandaboard.

Typically, gimbaled LIDAR systems utilize raster scan patterns, where LIDAR data is gathered one scan line at a time, with motion of the gimbal occurring between scans or at a relatively slow rate. This process can be very time intensive depending on the desired resolution and LIDAR FOV. With this type of scan pattern, as the ASV turns, objects in the LIDAR image can become distorted, as seen in Figure 6b – where the buoy appears tilted. This occurs because points in the depth image are not collected at exactly the same instant as when the LIDAR scans the environment. To overcome this issue, one of the innovations implemented in the presented gimbaled LIDAR system is the use of Lissajous-like scan patterns to allow a trade-off between speed and resolution without constraining the FOV [1].

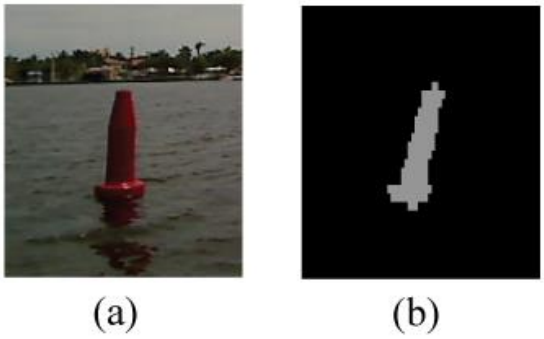

Figure 6: Example (a) camera and (b) depth images showing issues associated with motion.

The LIDAR and video sensors produce two outputs that must be fused: 1) Depth information, with corresponding gimbal and LIDAR angles, enabling the production of a depth image (shown in Figure 7a) 2) An RGB image (shown in Figure 7b). Figure 7c shows detail of the approximate RGB image region from (a).

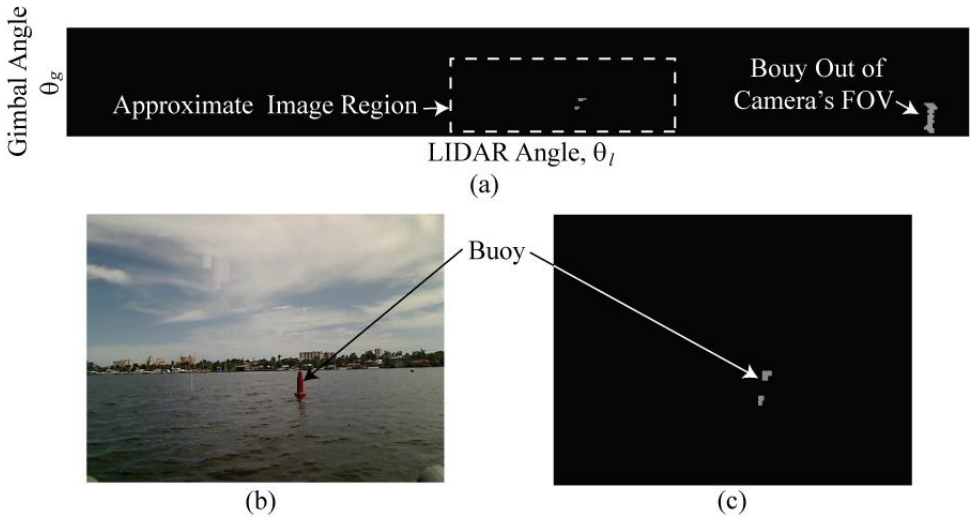

Figure 7: Example vision system images. (a) Depth image obtained from the LIDAR system. (b) RGB image obtained from the camera. (c) Detail image of the approximate image region in (a).

As an example, consider the problem of buoy identification. The LIDAR/Video fusion algorithm uses the depth image to identify objects of interest (not just buoys, but anything in the FOV of the LIDAR). It is advantageous to carry out the object identification in the depth image because floating objects are automatically isolated, both from the water (as the LIDAR is unable to return the distance to the water surface) and from the background (as LIDAR range is limited. As seen in Figure 7a this typically results in a small subset of points of interest (POI) in the depth image.

In order to fuse the LIDAR and Video images, the location of the POI needs to be transformed into RGB camera pixel coordinates. This is done by converting the LIDAR points to Cartesian XYZ coordinates, then translating the origin to that of the video camera, and finally calculating the pixel values through use of an intrinsic model of the video camera. This typically results in a sparse mapping of depth points to the pixel frame, as the camera has significantly higher resolution.

In order to better correlate the object being detected in the depth image with its corresponding object in the RGB image, the depth information is thresholded for a desired range and the remaining points are joined to make a continuous area using morphological operations (shown in Figure 8c). Mathematical details can be found in [14,15]

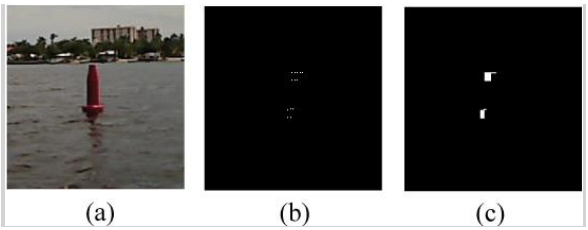

Figure 8: Example images showing (a) the original RGB image, (b) LIDAR data plotted in the camera coordinates, and (c) joined LIDAR data, creating a region of interest in the camera image.

Heavily coupled to the vision system is the SLAM. Without an internal map of its surroundings, the boat response can only be reactionary. That is to say, the vehicle may only react to sensor measurements (e.g., video, LIDAR) at the current time. To provide a higher level of functionality to the system, the vehicle must be able to leverage past sensor readings with current sensor data and form some estimate of important features in its environment. With an internal map of the environment, the vehicle can perform tasks such as path planning with obstacle avoidance, recursive color estimation for particular objects, and will have more accurate vehicle pose estimates. SLAM works to combine sensor measurements and control inputs to form an estimate about the robot's pose as well as features within a robotic environment. For the purpose of the boat, these features will be considered as buoys in the water. The particular variant of SLAM used in this implementation was FastSLAM [11,17].

V.II Ultra-Short Baseline SONAR System:

A unique component to this competition is the ability of the vehicle to detect and locate an underwater sound source. This is commonly accomplished by using an underwater SONAR system that is used to estimate the range and bearing to the source, in a body-fixed frame relative to the vehicle. Such navigation systems use underwater hydrophones, or underwater antennas, configured on specific baselines to determine the direction of arrival of an acoustic plane wave using either a time delay estimation or an inferometric process to correlate the signals. These systems include long baseline (LBL), short baseline (SBL), and ultra-short baseline (USBL) configurations – each with their own level of complexity and advantages [2]. For the competition, FAU has fully developed a USBL SONAR system that is independently packaged and contains its own launch and recovery system to raise and lower the array in and out of the water with the use of a linear actuator (Figure 10 - center).

The FAU USBL SONAR system is a split-beam array that contains a horizontal and vertical baseline that provides an azimuthal and vertical bearing to the source, respectively.

The system uses an inferometric process known as a split-aperture correlator to determine the analytical phase difference between two hydrophone signals on any given baseline and thus the bearing to the source. This is accomplished by exploiting the real form of the complex wave signal to produce an analytical imaginary form of the signal with the use of the Hilbert Transform. This type of filtering is a discrete convolution of the digitized data with the designed filter. The Hilbert transform for this application is linear time invariant (LTI) system with a transfer function defined as [3],

$$\hat{x} = H(f) = -j\, sgn(f)$$

The Hilbert Transform shifts the phase of all signals with negative frequencies

forward by 90° and all signals with positive frequencies back by 90°, such that the phase shift can be represented as [3],

$$\sigma_H(\omega) = \begin{cases} i = e^{j\pi/2}, & for\ \omega < 0 \\ 0, & for\ \omega = 0 \\ -i = e^{-\frac{j\pi}{2}}, & for\ \omega > 0 \end{cases}$$

The superposition of the real form and imaginary form allows one to extract the signal phase by using a phasor representation of the signal.

The phase shift at the center frequency of the narrowband signal is inserted so that the correlator output is responsive to the electrical phase difference.

The electrical phase difference is proportional to the target bearing. The phase difference, $d\Phi$, between the two given signals is a component, along with the signals carrier frequency, f_c, baseline length, b, and ambient acoustic sound speed, c, to estimate the direction of arrival of the incident plane wave relative to the baseline, such that [2,3],

$$\theta_i = \arccos\left(\frac{d\Phi}{\frac{2\pi f_c b}{c}}\right)$$

One of the most common and sometimes most difficult issues to overcome in bearing estimation is reducing the presence of multipath or reverberated acoustic waves caused by the environmental wave guide; the sea surface, nearby side walls or structures, and the sea bottom. These unanticipated acoustic waves cause destructive interference of the received signals of the hydrophones in the form of unwanted signal noise when trying to acquire a direct path ray from a received data set [7,8].

In this particular design, the array has been configured for a forward-down looking cone of sensitivity, as seen in Figure 9. This allows two features: 1) the array has a narrow cone of sensitivity to force signals in the array from a desired direction; 2) the array depression angle allows for optimal sensitivity of the system in the forward and downward directions relative to the vehicle for when homing far away and near/on top of the source. To reduce the multipath issue, many features have been incorporated including auto-variable gain tuner, increased detection gains to force only direct rays to be heard such that multipath rays are attenuated enough to be just below the threshold to be dismissed, enhanced coarse and finely tuned detection windows to extract first wave arrival information.

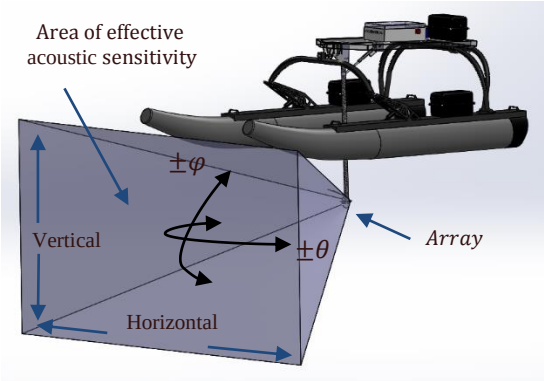

Figure 9: Isometric view of 3D cad model of WAM-V equipped with new in-house USBL positioning system design.

The current version of the system has a data acquisition component, digital filter, signal detector and bearing estimator. A dedicated data acquisition unit (National Instruments DAQ), is used to collect voltage samples from four separate channels simultaneously at 100,000 samples/sec. Each channel is the input for a hydrophone from the USBL array. The data are band pass filtered to remove ambient noise outside of the desired received bandwidth so as to maximize the accuracy of signal detections and bearing estimations. The digital filter is an FIR band pass filter with user selectable pass-band frequencies and 96 dB of stop band attenuation. The signal detector algorithm uses peak detection component operated with blocks of 10 ms at a time. If a signal maintains a peak above a provided detection threshold, then the signal is deemed to be "detected", while signals below this threshold are discarded. The signal detection threshold can be automatically scaled based on the ambient noise power and is recalculated every 8 seconds, thus providing a time-variable gain tuner for when the vehicle moves into new geographic areas with different ambient noise characteristics.

Figure 10 shows the current system assemblies. The mechanical packaging included restraining the NI DAQ system and TCS (Intel i5) processing board, as well as development of an in-house power regulation and signal interface board. This board is particularly designed to provide power to the necessary electrical components and harness the input signals from the hydrophone bus.

Figure 10: USBL positioning system acquisition and processing electronics (left); Automated launch and recovery system (center left); Actuation system for automated deployment and recovery of USBL positioning array (center right); USBL positioning array with horizontal and vertical baselines (right).

VI. Control Systems

Two distinct controllers for the vehicles were created according to the various challenges the Maritime RobotX Challenge presented. The first was a trajectory tracking controller for an underactuated vehicle that took in a series of waypoints and navigated the vehicle accordingly. The second was a station keeping controller for the overactuated case with azimuthing propellers - where the vehicle was given a particular waypoint and heading to maintain. The logic of switching between the two was dictated by the high-level planner. Figure 11 shows a breakdown of each of these controllers: the dotted line represents the vehicle desired trajectory, T_p and T_s are the port and starboard thrust with their respective directions.

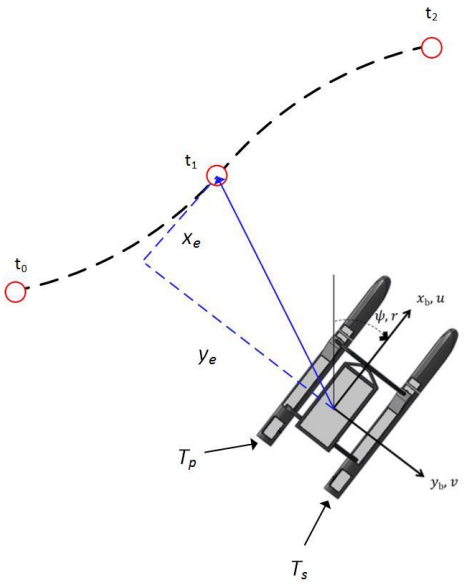

Figure 11: Controllers breakdown

The trajectory tracking controller was based upon a PD controller that acted upon the body-fixed error in position. As such, the equations of motion describing the controller could be summarized as:

$$\begin{bmatrix} x_e(t) \\ y_e(t) \end{bmatrix} = \begin{bmatrix} cos\psi & sin\psi \\ -sin\psi & cos\psi \end{bmatrix} \begin{bmatrix} x_d^g(t) - x^g(t) \\ y_d^g(t) - y^g(t) \end{bmatrix}$$

$$\begin{bmatrix} X \\ N \end{bmatrix} = \begin{bmatrix} K_{p,x} & 0 \\ 0 & K_{p,y} \end{bmatrix} \begin{bmatrix} x_e \\ y_e \end{bmatrix} + \begin{bmatrix} K_{d,x} & 0 \\ 0 & K_{d,y} \end{bmatrix} \begin{bmatrix} \dot{x_e} \\ \dot{y_e} \end{bmatrix}$$

where the two errors, x_e and y_e, were found by subtracting the vehicle's current position, x^g and y^g from the desired location of the vehicle at a certain time t in the inertial North-East-Down (NED) coordinate system. These errors and their derivatives were then multiplied by the PD gains K_p and K_d to determine the surge thrust of the vehicle X and the rotational component N. This system would cause the vehicle to turn towards the trajectory if it deviated away from it with an increase in the magnitude of its rotational torque N dependent on the extent of the sway error y_e. Likewise, any error in surge would cause the vehicle to speed up and continue following the trajectory at the prescribed rate. To deal with controller saturation and allocation in this underactuated case, the output of the controller X, N was then fed through an exponential function to manage thruster saturation.

$$X' = Xe^{-\beta|N|}$$

This new value of X' was used as the desired thrust for the vehicle.

The Station Keeping controller utilizes a Multi-Input Multi-Output backstepping controller [10]. This type of controller is ideal when unmodeled dynamics or environmental disturbances lead to significant deviations between simulated and experimental results [5]. Such a control scheme is essential when gain-scheduling techniques applied to linearized models cannot be applied. This is the case when trying to control surge and sway position (x,y) and yaw angle (ψ) simultaneously (station-keeping). A tracking surface was selected as:

$$s = \dot{\eta}_t + \Lambda \eta_t$$

Where η_t is the error in x,y,ψ and $\dot{\eta}_t$ its derivative. Λ is a diagonal design matrix based on Lyapunov exponent. The control law for station keeping then takes the following form:

$$\tau = M\ddot{\eta}_r + C(v)\dot{\eta}_r + D(v)\dot{\eta}_r * -K_d s - K_p \eta_t$$

Where M, C(v), and D(v) are the model matrices, K_p and K_d are the PD gains, $\dot{\eta}_r$ and $\ddot{\eta}_r$ are a defined virtual control vector and its derivative. The controller output, τ, corresponds to the forces and moment required to maintain the vehicle at the desired position and heading.

A Lagrangian multiplier method similar to that in [9] was used for control allocation. A cost function $J = \mathbf{f}^{\mathrm{T}}\mathbf{W}\mathbf{f}$ subject to $\boldsymbol{\tau} - \mathbf{T}\mathbf{f} = \mathbf{0}$ was used to solve for the control force vector broken down by components in the vehicle frame, $\mathbf{f}$. The other values in this function are the weight matrix $\mathbf{W}$, used to skew the result towards using the most efficient actuator, the transformation matrix $\mathbf{T}$ and the control force vector $\boldsymbol{\tau}$ as prescribed by the controller. Using a Lagrangian of $L(\mathbf{f}, \boldsymbol{\lambda}) = \mathbf{f}^{\mathrm{T}}\mathbf{W}\mathbf{f} + \boldsymbol{\lambda}^{\mathrm{T}}(\boldsymbol{\tau} - \mathbf{T}\mathbf{f})$, one can show that the solution for $\mathbf{f}$ reduces to $\mathbf{f} = \mathbf{T}_{\mathbf{w}}^{\dagger}\boldsymbol{\tau}$ where $\mathbf{T}_{\mathbf{w}}^{\dagger} = \mathbf{W}^{-1}\mathbf{T}^{\mathrm{T}}(\mathbf{T}\mathbf{W}^{-1}\mathbf{T}^{\mathrm{T}})^{-1}$ [11]. Due to the symmetry of the vehicle, the weight matrix $\mathbf{W}$ can be taken to be an identity matrix, which reduces $\mathbf{T}_{\mathbf{w}}^{\dagger}$ to the Moore-Penrose pseudo inverse of the transformation matrix, or $\mathbf{T}_{\mathbf{w}}^{\dagger} = \boldsymbol{T}^{T}(\boldsymbol{T}\boldsymbol{T}^{T})^{-1}$.

For this allocation system, an extended thrust representation is used, where each propeller's thrust is broken down into component forces and torques in the vehicle frame, i.e.

$$\boldsymbol{\tau} = \mathbf{T}\mathbf{f}$$

$$\boldsymbol{\tau} = \begin{bmatrix} 1 & 0 & \dots & 1 & 0 \\ 0 & 1 & \dots & 0 & 1 \\ -l_{y1} & l_{x1} & \dots & -l_{yn} & l_{xn} \end{bmatrix} \begin{bmatrix} F_{x1} \\ F_{y1} \\ \vdots \\ F_{xn} \\ F_{yn} \end{bmatrix}$$

for n number of actuators. Once the component force vector $\mathbf{f}$ is solved for using the pseudo inverse of the transformation matrix, it is trivial to apply a four-quadrant $arctan2$ function to find the rotation angle and calculate the magnitude of the thrust at each propeller.

Due to the fact that thrust characteristics are not precisely modeled within the allocation scheme, the resultant force and angle at each propeller is low-pass filtered with a user-set time constant

to maintain a feasible rotation rate in practice. Each propeller is capable of achieving a rotation from -45^o to 45^o – implying that a 180^o offset from those values are also attainable by reversing the propeller. A logic scheme is implemented on top of the allocation that stops the thrust if the allocation requests an unachievable angle, and reverses it if an angle from -135^o to 135^o is given. This approach produces a computationally efficient answer to the over-allocation optimization problem, capable of being implemented on an embedded system within the vehicle.

VII. Collaboration

The collaboration of FAU and VU to achieve the common goal of preparing the WAMV USV16 for the RobotX Maritime challenge was accomplished by splitting the efforts. Each university was able to efficiently devote their time towards their area of expertise. This allowed the entire team to reach goals that could have not been achieved individually. The collaboration between universities however also raised some non-typical challenges. One of the major milestones the team had to face involved system integration and testing, which became challenging due to the physical distance that separates FAU and VU. More specifically, the integration and collaboration between systems developed at different universities, by students with different backgrounds, required significant time and effort. In addition to this, the distance forced some the students to spend extended periods of time away from home, in order to allow testing. This also had an effect on the team budget, since travel and lodging for these students also had to be compensated. The entire team was however proud of the collaboration between universities and was able to successfully overcome all challenges involved.

As a firm belief that this is a student competition, the majority of the work was performed by the students of the team. However, in order to efficiently utilize technical expertise, in-house collaboration with engineering staff from both FAU and Villanova was an integral part of the project. More precisely, the machining of some major components such as thruster mountings, end caps, and various USBL deployment system components were built by a machinist at FAU. Expertise advice and service was utilized for the propulsion system design, system architecture design, electronic board design and assembly, system wiring and packaging by FAU's electrical and mechanical engineering staff. System integration and testing, along with the design of components and electronics packaging was handled by undergraduate and graduate students. All other non-technical tasks, such the website, the journal and the overall preparation for the competition were also fully handled by students. Finally, the advice of the faculty advisors (Dr von Ellenrieder, Dr Beaujean,

Dr Clayton and Dr Nataraj) was actively considered while making any decision.

VIII. Conclusion

Presented in this paper is the development of an autonomous shipboard system designed and equipped on the WAM-V USV16 for the inaugural Maritime RobotX Challenge in Singapore, 2014. Team WORX was able to develop and implement all the necessary components and required systems to attempt and succeed in all the major tasks of the competition. Future augmentations to the vehicle include enhanced mechanical and electrical components, as well as more developed high-level autonomy.

References

[1] Anderson J. W. and Clayton G., “Lissajous-like scan pattern for a gimbaled LIDAR.” *2014 Conference on Advanced Intelligent Mechatronics (AIM)*.

[2] Austin, Thomas. *The Application of Spread Spectrum Signaling Techniques to Underwater Acoustic Navigation.* Woods Hole, MA. Print.

[3] Burdic, William. *Underwater Acoustic System Analysis*. 2nd ed. Los Altos Hills, California: Peninsula Publishing, 2002. 361-380. Print.

[4] Haung S., Wang Z., and Dissanayake G., "Simultaneous Localization and Mapping: Exactly Sparse Information Filters," World Scientific Publishing Co., Danvers, MA, 1994.

[5] H. G. Sage, M. F. De Mathelin and E. Ostertag, “Robust Control of robot manipulators: a survery,” Int. J. Control, 1999.

[6] Huh S., Shim D. H., and Kim J., "Integrated navigation system using camera and gimbaled laser scanner for indoor and outdoor autonomous flight of UAVs," *2013 IEEE/RSJ International Conference on Intelligent Robots and Systems (IROS).*

[7] M. Miranda, P.-P. Beaujean, E. An, M. Dhanak, “Homing an Unmanned Underwater Vehicle Equipped with a DUSBL to an Unmanned Surface Platform: A Feasibility Study”, Proc. of the MTS/IEEE Oceans’2013, San Diego, CA, Sept. 2013, pp. 1-10.

[8] M. Miranda, “Mobile Docking of Remus-100 Equipped with USBL-APS To An Unmanned Surface Vehicle: A Performance Feasibility Study”, M.S. Thesis, Florida Atlantic University, Boca Raton, FL, May 2014.

[9] O. J. Sordalen, "Optimal thrust allocation for marine vessels," *Control Eng. Prac.,* vol. 5, no. 9, pp. 1223-1231, 1997.

[10] T. I. Fossen and J. P. Strand, “Tutorial on nonlinear Backstepping: Applications to Ship Control,” Modeling, Identification and Control, 1999

[11] Thrun S., Burgard W., and Fox D., *Probabilistic Robotics*, Cambridge, The MIT Press, 2006

[12] Wulf O. and Wagner B., "Fast 3d scanning methods for laser measurement systems," *2014 International conference on control systems and computer science (CSCS14).*

[13] Yoshida T., Irie K., Koyanagi E., and Tomono M., "3d laser scanner with gazing ability,” *2011 IEEE International Conference on Robotics and Automation (ICRA).*

[14] Anderson Lebbad, Nicholas DiLeo, Chidananda Matada Shivananda, Frank Ferrese and C. Nataraj, "Probabilistic Vision Based Guidance & SLAM for Autonomous Surface Vehicles", *Naval Engineers Journal*, December 2014.

[15] J. Wes Anderson, Anderson Lebbad, C. Nataraj and Garrett Clayton, "An Integrated LIDAR/Video Vision System for Autonomous Surface Vehicles", *Naval Engineers Journal*, December 2014.

[16] Edward Zhu, Dylan DeGaetano, GinSiu Cheng, Priya Shah, Michael Benson, Gus Jenkins, Frank Ferrese, and C. Nataraj, "An Experimental Autonomous Surface Vehicle With Vision-Based Navigation, Obstacle Avoidance & SLAM", *Naval Engineers Journal*, December 2014.

[17] Nicholas DiLeo, “FastSLAM: Mapping for an Autonomous Surface Vehicle,” Independent Study report, Villanova University, May 2014.